Spring 5-2018

The Effect of Material Variability on the Deflection of Bamboo Fly Rods

Bennett R. Scully
University of Maine

THE EFFECT OF MATERIAL VARIABILITY ON THE DEFLECTION OF BAMBOO FLY RODS

by

Bennett R. Scully

A Thesis Submitted in Partial Fulfillment

of the Requirements for a Degree with Honors

(Civil & Environmental Engineering)

The Honors College

University of Maine

December 2018

Advisory Committee:

Edwin Nagy, Lecturer of Civil & Environmental Engineering, Advisor

Eric Landis, Professor of Civil & Environmental Engineering

Roberto Lopez-Anido, Professor of Civil & Environmental Engineering

Mimi Killinger, Associate Professor, Honors College

Craig Diegel, Reverence Fly Rods

ABSTRACT

This study tested and compared the theoretical effect of variability in modulus of elasticity versus rod taper in the "action" of bamboo fly fishing rods. Action is a rod's tendency to flex in specific areas when loaded and the extent to which it deforms in that area. MATLAB functions were scripted to plot the large deflection of bamboo fly rods in order to model the action of a rod given various properties. The bamboo fly rod was considered to be a cantilever beam with a point load acting on the end, and large deflection considerations had to be made. Materials testing was performed on bamboo to obtain an expected distribution of modulus of elasticity values to be used within the function. Various rod taper dimensions were retrieved from David Ray's Taper Library and used in the deflection function. This study observed strictly the static deflection of bamboo fly rods in the considerations of material variability's effect on fly rod action. Material variability in bamboo was found to have a significant impact on the action of a fly rod with respect to taper.

ACKNOWLEDGEMENTS

I would like to express my sincere thanks to Edwin Nagy, my thesis advisor, for providing me with the insight and assistance necessary to complete this endeavor, to the progenitor of this project, Craig Diegel, to Fred Kretchman for providing the bamboo samples needed for my materials testing, to William Davids and the Civil & Environmental Engineering Department for providing funding for said bamboo samples, to Eric Landis and Roberto Lopez-Anido for sitting on my committee and for providing

assistance, and to Margaret Killinger for supporting me throughout my reading list process.

TABLE OF CONTENTS

LIST OF FIGURES

LIST OF TABLES

CHAPTER 1: INTRODUCTION

Fly fishermen use many terms to describe how a rod feels when in use, the most common term being “action.” Although action is such an important aspect of the fly rod, there is no industry standard for classifying and describing how a rod flexes and feels when in use. It is common belief that the action of a rod refers to the stiffness, tendency to flex in specific areas, and the speed of recovery. Rod action is affected by the taper of the rod and the stiffness of the materials used, however, taper is widely considered to be the dominating factor in action (Kretchman, 2017). Stiffness is determined by the properties of the bamboo that make up the rod, meaning that this stiffness can vary along the rod, and can even vary within the same rod depending on the direction of loading (Orvis). Considering that bamboo is a natural material, there can be significant variability in the material properties between individual bamboo culms and variability within an individual culm. This project aims to reveal the effect that material variability has on fly rod action. Particularly of interest is if material variability has a significant impact on rod action compared to rod taper, or if rod taper is dominant enough that material variability can be ignored in the design of fly rods.

Fly rods have been constructed out of a variety of materials throughout history. The first material used was wood, which advanced to bamboo cane rods, and eventually split bamboo rods (Admin, 2009). Fiberglass rods were introduced in the 1940’s, followed by carbon fiber rods in 1976. Fiberglass was the most common of these materials because it most accurately replicated the action of bamboo rods. Graphite was introduced two decades later, which is now the most common material to be used in fly

rod manufacturing (Admin, 2009). These materials allow for fast manufacturing and consistent rods, however, split bamboo fly rods are considered by many to be an essential addition to any avid fly fisherman's collection. Bamboo is a member of the grass family known for its impressive strength to weight ratio, having a larger longitudinal compressive strength to weight ratio than wood, concrete, or brick (Fan, H., & Fan, C.). A testimony to its strength, bamboo is commonly used as scaffolding during construction projects in parts of the world.

Bamboo has been used as a material in fly fishing rods for centuries. Tonkin Cane (Arundinaria amabilis) is the most common species of bamboo used in the making of fly fishing rods, being one of the strongest species (Sweetgrass Rods). This can be attributed to its large amount of high-density fibers and flexibility in relation to other species of bamboo (Sweetgrass Rods). Bamboo grows in culms, consisting of three layers - a thin outer wall called the enamel, a middle layer of dense fibers which give bamboo its strength, and an inner layer of weak pith (Monahan, 2016). In order to form the fly rod, the manufacturer splits culms of bamboo into triangular sections and glues the lengths together to create a typically hexagonal cross section.

Like any other fly fishing rod, whether created using graphite or fiberglass, bamboo rods behave differently with respect to each other. This variability in behavior is due to two factors: the geometry of the rod, and the material used. The geometry of the rod refers specifically to the taper, or the reduction in thickness along the length of the rod. The other factor, the material used, is a function of the properties of the individual strips used to compose the rod.

The variability in behavior is primarily due to bamboo being a natural material. Each individual strip of bamboo will have different material properties based a multitude of factors, including the age of the culm, the longitudinal and latitudinal location on the culm, the presence of an imperfection such as a node along that section, the ratio of high density fibers to pith in that strip, the moisture content, and more (Schott, 2006).

Figure 1.1: Bamboo culm compared to glued hexagon (Cameron)

Fly rod manufacturers reduce this variability through actions such as deliberately orienting nodes in a variety of particular patterns, heat-treating the bamboo culms to gain a more consistent water content, and using strips that all originate from a single culm to make an individual rod.

The action of a rod is important to the fisherman based on personal preference and desired use, as each rod has its advantages and disadvantages for any given application. Generally, a fisherman will field test a rod before buying it to ensure it has the desired attributes. It would be helpful for rod makers to be capable of predicting the action of a rod prior to building it. Therefore, it would be beneficial to understand magnitude of the effect of material variability on the action.

Fly rod action is a dynamic, multidimensional concept, however, this thesis will focus strictly on the static deflection of bamboo fly rods. MATLAB was used to model

the static large deflection of a fly fishing rod. The rod was treated as a cantilever beam fixed at one end, with a point load acting vertically at the tip. The point load represents the force acting on the tip of the rod through the loaded fishing line. The modulus of elasticity was measured in various bamboo samples. Rods of various tapers were modeled, and the deflection of these rods using elasticity values corresponding with the materials testing results were graphed and presented. Future work must be done to incorporate dynamic considerations into the modeling of bamboo action, and to gain a better understating on bamboo variability. This thesis is the first component of the project, which aims to accurately model the static motion of a bamboo fly rod in order to predict the action of a rod given specific components such as length, taper, and the modulus of elasticity of each individual strip. Given this capability, we hope to be able to determine the extent to which rod taper and material variability affect the dynamic action of a fly rod with respect to each other.

CHAPTER 2: MATERIALS & METHODS

2.1. MATERIALS TESTING

Testing was conducted in order to gain insight on the modulus of elasticity of bamboo and the variability in the material to be used in the modeling of bamboo fly fishing rods. Tensile testing was performed on triangular bamboo strips. Bending tests were performed on hexagonal bamboo strips, which are created by gluing six triangular strips together. The purpose of this test was to collect a baseline of bamboo elasticity and expose a relationship between variability in bamboo strips and variability in compound bamboo hexagonal strips. It was predicted that the combination of six triangular strips into a hexagonal section would produce a smaller deviation in elasticity compared to the individual strips.

2.1.1. TENSILE TESTING

Tensile testing was performed on bamboo strips of triangular cross-section. This was done for strips with bases of two different widths, one width representing a strip that would be used in the middle section of a rod, and the other representing a strip that would be used in the butt section of a rod. All strips were heat treated by the rod manufacturer. The strips were likely not from the same culm. Fifteen strips of each size were tested at three locations along the length of each strip, resulting in forty-five readings for each strip size. The strips were cut to seven inches in length and marked in the middle and at points ¾ of an inch above and ¾ of an inch below the middle. A caliper was used to measure the height, H and base, B of the bamboo strips at the marked points as shown in Figure 2.1.

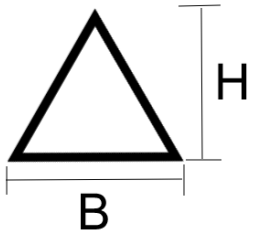

Figure 2.1: Cross-sectional view of triangular bamboo strip

The caliper is accurate to a one-hundredth of an inch, although that does not account for human error. Area, A was calculated as follows: $A = \frac{1}{2}BH$.

An Instron was used to execute these tensile tests. The bamboo samples were slightly too narrow for the Instron grips, so small aluminum plates with slight abrasions were used to fill the gap to prevent slipping. A ½ inch long strain gauge was used at the three marked points along the strips. The speed of test was 0.015 mm/min. Each test ran for approximately 0.75 minutes. Strain readings were set to begin recording at a load of 20 lbs to avoid initial non-linear results. Strain was measured at the middle of each strip for loads from 20 - 90 lbs. The test was then stopped, the strain gauge was relocated to the bottom mark, and the strain was measured from 90 - 120 lbs. The test was stopped again, and the gauge was relocated to the top mark, and the specimen was tested form 120 - 150 lbs. A data reading was made every 0.2 seconds. The readings were observed and confirmed to be linear during these tests to ensure there was no slipping or yielding during the experiment.

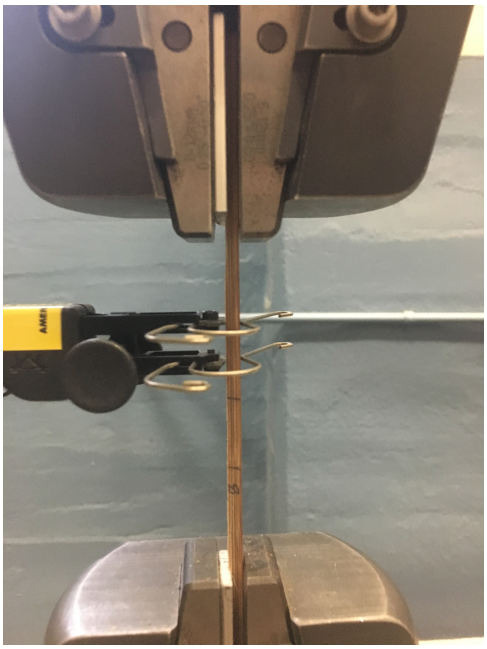

Figure 2.2: Tensile testing setup

2.1.2. 3-POINT BENDING TESTING

Three-point bending tests were performed on bamboo specimens of hexagonal cross-section of three different sizes using an Instron 8871. WaveMatrix was the program used to collect the data. This hexagonal cross section is typical in split culm bamboo fly rods, and is created by binding six triangular strips together using resin. An experienced bamboo fly rod maker, Fred Kretchman of Kretchman Fly Rods, provided these samples, all of which were heat treated by Fred. It is likely that the strips used to make these hexagonal pieces originated from different culms. The specimens were untapered, having approximately the same width across their lengths, and had a length to width ratio of at least 15:1 to minimize the effect of shear deformation in relation to bending deformation during the test. This promotes an accurate calculation of modulus of elasticity from the test results. The sections were measured in the middle, and at both ends using calipers and the measurements were averaged. For the butt-sections, the platform was set to a

span of 190 mm, was run until 2 mm of deflection was achieved, and was loaded at a rate of 1 mm of deflection per minute, resulting in a test time of approximately 2 minutes. The span for the middle sections was set to 142 mm, running until a deflection of 1.5 mm was achieved, with a rate of 1 mm/min, resulting in a test time of approximately 1.5 minutes. The span for the tip sections was set to 70 mm, running until a deflection of 1 mm was achieved, with a rate of 1 mm/min, resulting in a test time of approximately 1 minute. Data was recorded every quarter of a second. Fourteen tip-sections, sixteen mid-sections, and twelve butt-sections were tested in bending.

2.2. MATLAB MODELLING

The program MATLAB was used to model various mathematical problems. Several functions were written, including code that modified the transform section method for determining an effective modulus of elasticity and moment of inertia of a hexagonal cross section, and a function the determines the large deflection of a bamboo fly rod with a given taper and modulus of elasticity. These models were written to gain insight in the effect of material variability on the action of bamboo fly rods.

2.2.1. TRANSFORM SECTION

Transform section is a method of analysis often used in structural engineering in order to determine an effective modulus of elasticity of a composite beam containing components of varying material properties. It is generally used on beams comprised of rectangular sections stacked upon one another. A MATLAB function was created to use the transform section method to produce an effective modulus of elasticity and moment of inertia for a hexagonal cross-section composed of six triangular strips of given base width and an individual modulus of elasticity for each strip.

Since the transform section method is meant to work for rectangular components, the hexagon had to be treated as a stack of rectangles that compose the general shape of the hexagon. The hexagon was broken into *n* rectangular sections, each of which was composed of a certain percentage of the corresponding triangles pertaining to the location of the rectangular strip within the hexagon.

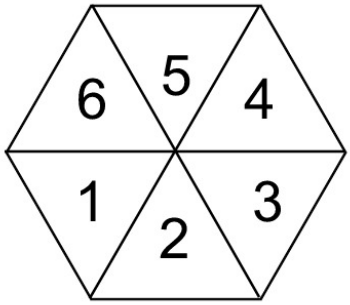

Figure 2.3: Hexagon orientation

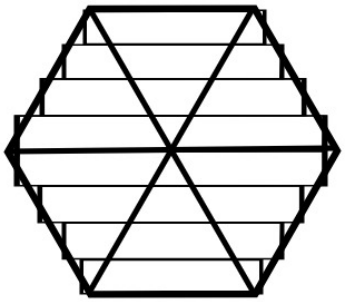

Figure 2.4: Hexagon when n = 8

Figure 2.4 shows an example of a hexagon being represented by eight rectangles. It is apparent that each rectangle is composed of a different percentage of each triangle, for example, a large percentage of the bottom rectangle in Figure 2.3 is composed of triangle 2, while a smaller portion is composed of triangles 1 and 3. The rule of mixtures was used to produce a weighted average modulus of elasticity for each layer. Through

this process the individual modulus of elasticity for each of the three triangles that compose any given rectangle were multiplied by a factor relative to the percent composition of that rectangle. Given percent composition, T_j, and modulus of elasticity, E_j, the calculation for resultant modulus of elasticity for a rectangle, Er_i is as follows: $Er_i = \sum_{j=1}^{n} E_j T_j$.

Once the triangles are divided into their equivalent rectangles, the function uses the standard transform section method to calculate a resultant modulus of elasticity. The parallel axis theorem is used to calculate the moment of inertia. As the number of rectangles, *n* increases, the function calculates a modulus of elasticity and moment of inertia that is more representative of the hexagon. A convergence test was performed and it was determined that *n* values of 50 or greater yielded results that had insignificant changes as *n* continued to increase. We used n=50 for all models.

Moment of inertia is calculated by first determining a transformed width, *b* for each rectangle, which is the width at the center of that section, *n*. These widths are multiplied by the height, *h* of each slice, resulting in transformed areas for each rectangle. The distance of the centroid of each rectangle to the base is calculated, and the values of this vector are multiplied by the respective rectangle transformed area. The neutral axis of the hexagon is determined by dividing the sum of the above calculation by the sum of the transformed areas. The neutral axis is subtracted from the distance from the base to centroid of each rectangle, and the result is squared. This value is multiplied by the tributary width for each rectangle, the product of which is I_I. The resultant moment of inertia, I, for the hexagonal shape is the sum of I_I and I_o, where $I_o = \frac{1}{12} bh^3$.

2.2.2. LARGE DEFLECTION MODELS

Two MATLAB functions were written to calculate and present the equilibrium deflected shape of a bamboo fly rod. These two functions follow much of the same procedure and many of the same assumptions. In order to represent this deflection, the rod was considered to be a cantilever beam, meaning that it was fixed on one end, while the other end was free. A load is applied perpendicularly to the long axis of the rod on the free end of the beam to simulate the static loading of a fly rod. The two models are based on the Euler-Bernoulli theory, which relies on small deflection assumptions. For one, it is assumed that the length of the beam remains constant through the deflection, and therefore, the load is acting at a point at a constant distance from the beam's fixed end, which results in a constant moment. It is also assumed that plane sections remain plane and normal to the axis. The following equation represents the relationship between curvature, slope, and deflection:

$$k = \frac{v''}{[1+(v')^2]^{3/2}} = \frac{M(x)/EI}{[1+(\theta)^2]^{3/2}} \qquad [1]$$

where k is curvature, θ is the slope, and v is the deflection of each section, $M(x)$ is the moment at location x along the rod, and EI is the product of modulus of elasticity and moment of inertia at that location on the rod. During small deflection, the slope of a given beam will be extremely small. Looking at equation [1], we see that if we have a very small value for slope, and we then square this value, the result is that element of the equation approaching zero. This effectively makes the denominator equal to 1, or we find that curvature is equal to the second derivative of deflection, or $M(x)/EI$. In the first model we created, we consider the slope to be negligibly small, so we make the approximation that $k=M(x)/EI$. The second function we made does not make the

assumption that slope can be considered to be zero. In this function we make an exact calculation of slope using equation [1].

The functions calculate the total tip deflection, and the rod's deflection along its length. It plots the final deflected shape of the beam, illustrating the rod's tendency to flex at specific points along the rod. The function requires inputs for the load at the end of the beam, *P*, the number of nodes along the beam, *n*, a value for modulus of elasticity, *E*, and the dimensions for the taper of a given fly rod.

The number of nodes effectively divides the beam into that amount of sections of equal length. Given the taper dimensions, the function uses linear interpolation to calculate X and Y coordinates for each node along the length of the beam. The initial shape of the beam is a horizontal cantilever, with y-coordinates and slope, θ, of each section being equal to 0. The moment of inertia for a hexagon is calculated at each node along the length of the beam using the following equation, where *h* is the height of the hexagon when oriented flat side down:

$$I = \frac{5\sqrt{3}}{144} h^4 \qquad [2]$$

The function creates a vector of values of the product of moment of inertia and the modulus of elasticity at each node, *EI*.

A loop within the function runs, within which curvature, ρ, is calculated for each segment of the beam given the applied load *P,* the length of the segment for which the load is being applied *(X(n) –X(i)),* and *EI* using the following equation where *P* multiplied by the distance from the load is equal to the moment, *M(x)*:

$$\rho = P\frac{X(n)-X(i)}{EI(i)} = \frac{M(x)}{EI} \qquad [3]$$

The slope, θ, of each segment is calculated using the curvature from the previous iteration, ρ, the segment length, *ds*, and adding the previous slope:

$$ds = \frac{l}{n-1} \quad [4]$$

$$\theta_i = \rho_{i-1} * ds + \theta_{i-1} \quad [5]$$

The coordinates of the present node is then calculated using trigonometry as shown below:

$$X_i = X_{i-1} + ds * \cos(\theta_{i-1}) \quad [6]$$

$$Y_i = Y_{i-1} + ds * \sin(\theta_{i-1}) \quad [7]$$

The above process within the loop effectively performs a double integration of curvature at each node to produce the deflection at each point. The use of nodes allows us to have a smooth interpolation of taper along the length of the rod. The assumption that plane sections remain plane is satisfied due to the use of nodes because the beam segment between nodes, *ds*, has a curvature small enough that it can be considered plane when using a large value of *n*.

Every time the loop runs, new X and Y coordinates for the nodes of the rod are calculated. Every iteration of the loop uses the X and Y coordinates from the previous iteration. The basis for the small deflection assumption that there is no change in length is that a change in length would result in a change in moment due to the point load being in a different location since the moment is equal to load times length. The change in length is demonstrated below:

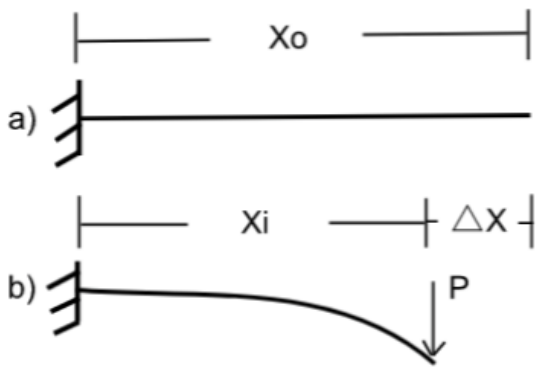

Figure 2.5: Change in length during large deflection

We can see that a change in length in the X-direction will cause a change in moment, and will therefore affect the calculation of deflection. This loop runs until the percent change in the deflection of the tip of the current iteration from the previous iteration is less than 0.1%, which is when the system effectively reaches equilibrium.

Considering the first iteration, we see that the curvature should be equal to zero because the beam is un-deflected, however, the length of the beam is at it's greatest, leading to a high calculation for the moment. This leads to an overestimation for the initial curvature because it should be equal to zero, leading to an overestimation of deflection. The new beam coordinates based on this deflection are then used in the next iteration. The length of the beam, based on these coordinates, is shorter than the actual length of the beam, leading to an under calculation of moment, leading to an under estimation of deflection. These coordinates are used in the next iteration, leading to an overestimation of deflection, however, not as much of an overestimation as in the first iteration. This process continues, resulting in an alternation of overestimations and underestimations between iterations, each iteration reaching a value more representative of the correct deflection of the beam. Given this mechanic, the function finds the

deflected shape of the rod that satisfies equilibrium of the internal moments at each node due to the external load and curvature. Equilibrium is when the curvatures due to moments based on the actual beam shape predict the actual deflected beam shape.

The two deflection models were run within a script that plots $[L - \Delta X]$ by $\left[P\frac{L^2}{EI}\right]$, as well as ΔY by $\left[P\frac{L^2}{EI}\right]$ on the same graph. The results were compared to the published findings of Dado Al-Sadder. Contrary to theoretical predictions, it was determined that the function based on small deflection assumptions yielded results closer to Al-Sadder than the function containing the extra consideration in the calculation of curvature.

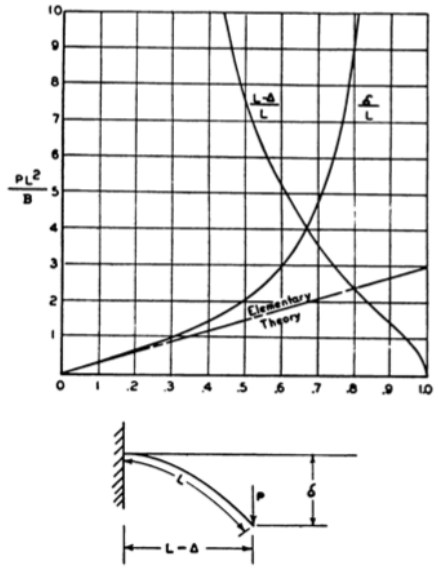

Figure 2.6: Dado Al-Sadder large deflection theory plot (Bisshopp, 1945)

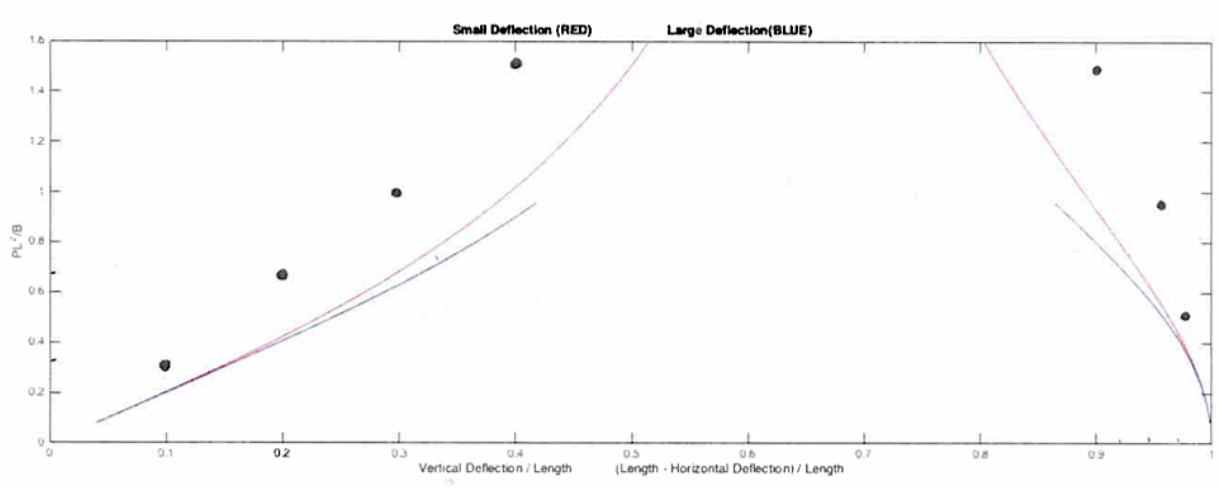

Figure 2.7: Rod deflection model comparison to Dado Al-Sadder (Bisshopp, 1945)

Values from Figure 2.6 were scribed onto the Figure 2.7, presented above. Figure 2.2 displays the results of the two large deflection models we made to determine which one was more consistent with the published findings of Dado Al-Sadder. From this figure we can see that the model based on small deflection assumptions diverges from the published values slower than the model with the added large deflection considerations. We used the former model in our tip deflection analysis because of this. We also see that the large deflection function ceases to work after $\frac{PL^2}{B}$ values of approximately 1 are reached, which is another reason we relied on the model based on small deflection assumptions.

CHAPTER 3: RESULTS AND DISCUSSION

Tensile and 3-point bending tests were conducted. The results from these tests were analyzed and used in the MATLAB models in order to draw conclusions on the correlation between material variability and the deflection of bamboo fly fishing rods.

3.1. TENSILE TESTING RESULTS

The tensile tests resulted in elasticity values similar to those published in Schott's *Bamboo in the Laboratory* (2006). As stated, tensile tests were performed on two different sizes of bamboo, mid-section strips and butt-section strips. Fifteen of each sized sample were tested each at three different points along their lengths, resulting in a total of 45 readings for each size. A sample load-deformation curve is presented below:

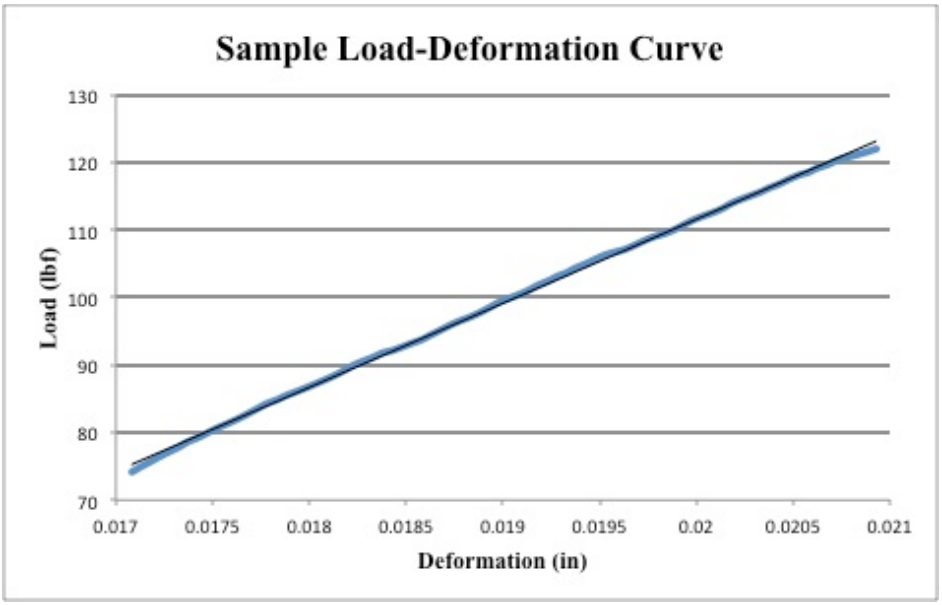

Figure 3.1: Sample tensile load-deformation curve

Modulus of elasticity, E is given by the quotient of stress, σ over strain, ε:

$$E = \frac{\sigma}{\varepsilon} = \frac{P \times L}{A \times \Delta L} \quad [8]$$

where stress is equal to the product of applied load in tension, *P* and the length that deformation was measured over, *L*, and strain is equal to the product of cross-sectional area, *A* and the change in length, or deformation, *ΔL*.

Data sets were analyzed to determine an average elasticity of 5.67×10^6 psi with a standard deviation of 8.25×10^5 psi for the mid-section bamboo strips. Butt-section strips were determined to have a mean elasticity of 4.62×10^6 psi, and a standard deviation of 1.33×10^6 psi.

Table 3.1: Tensile materials testing results

Specimen Size	Mean MOE (psi)	Standard Deviation of MOE (psi)
Mid-Section	5.99×10^6	8.25×10^5
Butt-Section	4.62×10^6	1.33×10^6

Histograms of the elasticity results are presented below:

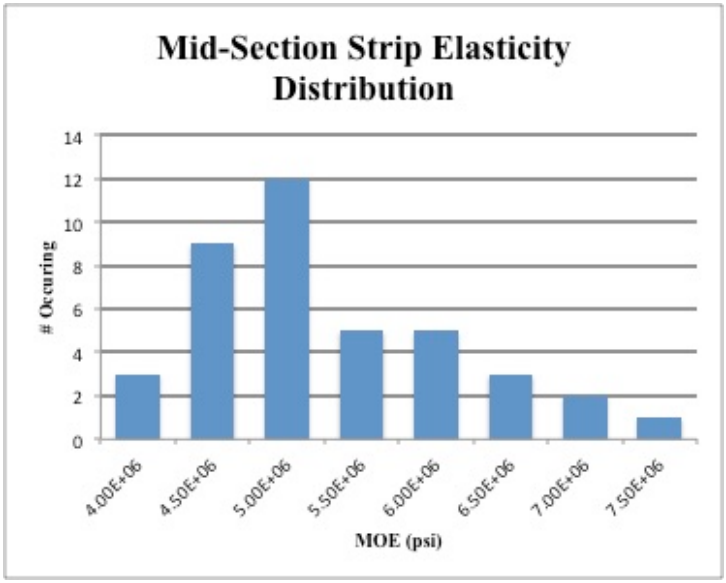

Figure 3.2: Mid-section elasticity histogram

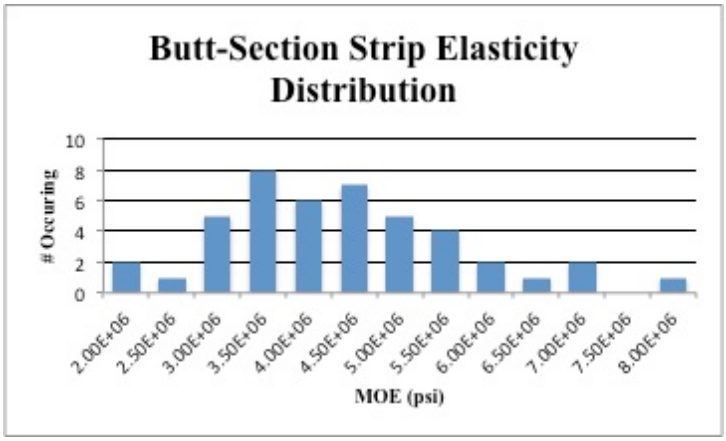

Figure 3.3: Butt-section elasticity histogram

The histograms are asymmetric and not smooth. This may be a result of having too small of a sample size. We make the assumption that these data sets have a normal distribution.

Analyzing this data, we found that the mid-section strips have an elasticity that is 18.5% higher than the butt-sections. This is likely due to the presence of a higher percentage of dense power fibers in the mid-section strips, and a smaller percentage of pith relative to area. The butt-section strips are composed of a greater percentage of pith, leading to a lower elasticity. The standard deviation for the butt-section strips is 38% greater than the standard deviation for the mid-section strips. This can likely be attributed to the variance in percentage in power fibers between the two sized strips as well (Schott, 2006).

A t-test was conducted in order to determine the statistical significance of the difference in elasticity between the mid-section and the butt-section strips. A p-value of 0.0058 was obtained, which means that this difference in elasticity between the two sized strips is highly statistically significant. This result means that the difference is likely to be valid and representative of the population.

The results from this test appear accurate, however, it is recommended for future tests that the load be reset after every test. Instead of loading in consecutive increments for the three marks on a bamboo strip, the load should be reset every time the strain gauge is moved. Although the graphed results appeared linear, it is possible the slopes of these increments were affected by the increase in load throughout the three tests. This would certainly be avoided if the load was reset for every test. Another important consideration for future work is to determine the effect of the presence of a node along a bamboo strip.

3.2. 3-POINTS BENDING TEST RESULTS

The bending tests yielded results that were not expected. Having analyzed the data, it became evident that there was vast variation between the different sized samples. It was predicted that the tip sections would yield the highest elasticity, due to them consisting of almost strictly dense power fibers. The elasticity was predicted to decrease slightly as the sections increased in size due to the increased percentage of the strip being composed of pith. Elasticity was calculated in bending using the following relationship between length, L, moment of inertia, I, and the slope of applied load over deformation, k:

$$E = \frac{kL^3}{48I} \quad [9]$$

The calculated average and standard deviation elasticity values are as follows:

Table 3.2: 3-point bending materials testing results

Specimen Size	Mean MOE	Standard Deviation of MOE
Tip-Section	1.51×10^6	2.52×10^5
Mid-Section	3.05×10^6	5.27×10^5
Butt-Section	4.25×10^6	3.25×10^5

Comparing this to the tensile results, these hexagonal bending results represent an inverse relation between size and elasticity. The calculation of the elasticity of these sections was corroborated using multiple methods, reducing the risk of these unexpected results being due to calculation error.

A one-way ANOVA test was used to evaluate the statistical significance of these findings. This method is used to analyze the variance of three of more independent groups. An assumption that must be made to use this method is that the individual groups are normally distributed. The following histograms are assumed to represent normal distributions, but with lack of a sufficient number of samples.

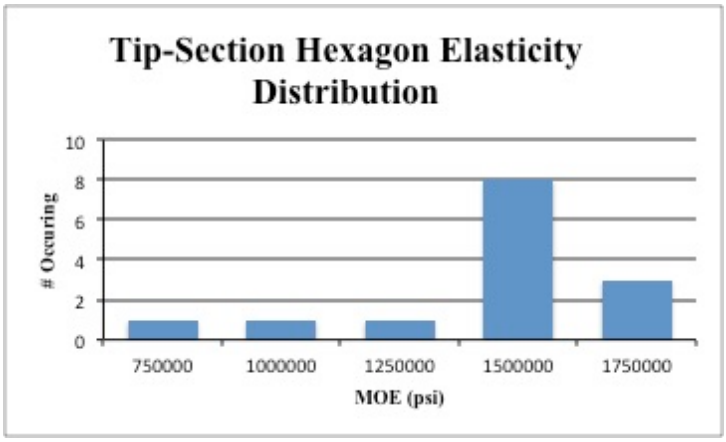

Figure 3.4: Tip-hexagon histogram

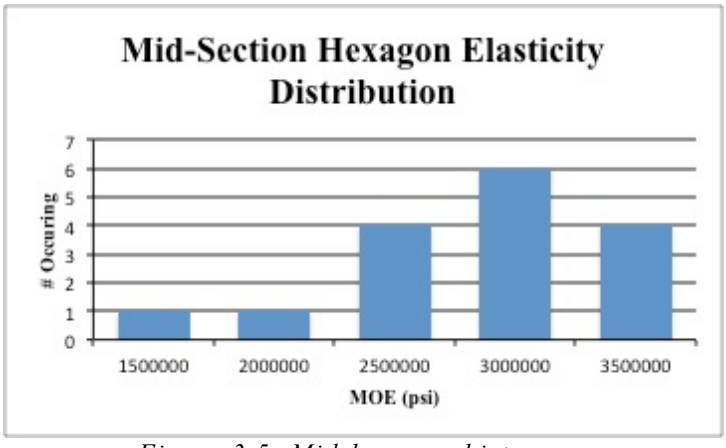

Figure 3.5: Mid-hexagon histogram

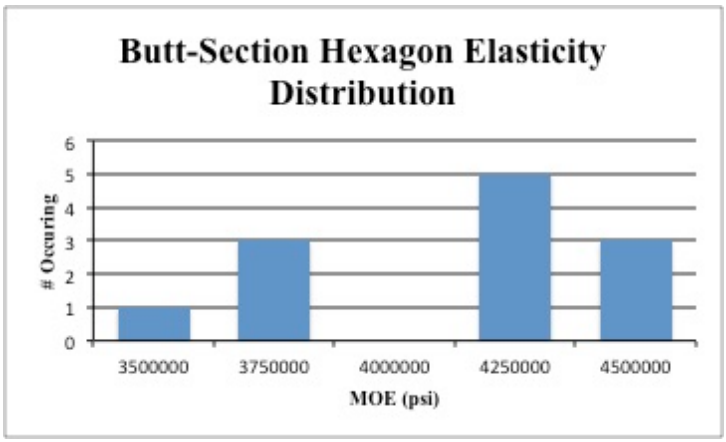

Figure 3.6: Butt-hexagon histogram

The ANOVA test resulted in a p-value of $1.05x10^{-19}$. A p-value of any less than 0.005 is generally considered extremely statistically significant. The calculated p-value is sixteen orders of magnitude smaller than 0.005, meaning there is nearly no chance that the results are due to a statistical fluke.

This narrows down the potential explanations for these unexpected results. One possible reason is that there was a mistake in the methods of the testing, or a mistake was made during the testing process. Another potential explanation is that the results are correct, however, the fundamental reason for these results is being overlooked. For example, the bonding agent used to glue the strips together was considered as a potential influence on the results; however, this was deemed unlikely to be a large factor due to the coat of glue being minimal and the fact that the same glue was used on all samples.

It is recommended for future testing that all bamboo samples originate from a minimal amount of culms, and the origin of the samples is tracked so variability from the samples coming from different culms can be ruled out as a factor affecting the results. If this can be determined to be a non-factor, then any unexpected results can be associated with a mistake in the methodology or the results may be considered to be accurate, even if not expected.

3.3. TRANSFORMED SECTION MODEL RESULTS

The transform section function was used within a script in order to determine the effect that combining six individual strips into a hexagon had on the variability of the material. The mean and standard deviation values presented in Table 3.1 were used in this script. Six hundred strips were generated within the script, each of which was randomly assigned a modulus of elasticity within one standard deviation of the mean. These six hundred strips were run through the transform section function, six at a time, resulting in one hundred hexagonal sections with a calculated effective modulus of elasticity for each. The mean and standard deviation modulus of elasticity were calculated for these hexagons. This process was executed for the mid section strips and butt section strips.

When comparing the values of mean and standard deviation between mid-section strips and hexagons, it was found that the mean remained unchanged between having six hundred individual strips, and having one hundred hexagons, each containing six of the aforementioned strips. However, when compiled into hexagons, the standard deviation decreased from 8.23×10^5 psi to 4.85×10^5 psi. This represents a 41% decrease in standard deviation. Similarly, the mean remained constant for the butt-section strips, while the standard deviation decreased from 1.33×10^6 psi to 7.48×10^5 psi. This represents a 43.8% decrease in standard deviation.

To explain these results, the relationship: $SD_{new} = \frac{SD}{\sqrt{n}}$ was used to determine the expected standard deviation of the hexagon when combining the six individual strips, where *n* is the number of independent elements being combined, or 6, in this case, *SD* is the standard deviation of these six individual strips, and SD_{new} is the expected standard deviation of the resultant when these six strips are combined as one. This method is

assuming that all six strips are of equal influence, for example, if the six strips were laid side by side. In the situation of this hexagonal shape, the bottom and top triangles will have more influence on the modulus of elasticity than the other four strips. Given these two relationships, the hexagonal results are expected to be somewhere between the expected results where n=2 and n=6. When n = 6, a mid-section SD_{new} of $3.37x10^5$ psi and a butt-section SD_{new} of $5.43x10^5$ is expected. When n = 2, a mid-section SD_{new} of $5.82x10^5$ psi and a butt-section SD_{new} of $9.4x10^5$ is expected. The new standard deviation value produced from this function is corroborated due to it being between the expected new standard deviations when n = 2 and n = 6 as tabulated below:

Table 3.3: Transform section model results

Elasticity (psi)	Mid-Section	Butt-Section
Strip Mean	$5.99x10^6$	$4.62x10^6$
Hexagon Mean	$5.98x10^6$	$4.72x10^6$
Strip Standard Deviation	$8.23x10^5$	$1.33x10^6$
Hexagon Standard Deviation	$4.85x10^5$	$7.48x10^5$
Expected Standard Deviation (n = 2)	$5.82x10^5$	$9.4x10^5$
Expected Standard Deviation (n = 6)	$3.37x10^5$	$5.43x10^5$

3.4. LARGE DEFLECTION MODEL RESULTS

The deflection model was run with the intentions of displaying the magnitude of the effect of material variability on the deflected shape of a bamboo fly rod. In order to do so, the rod deflection function was run for a variety of tapers. The three calculated deflections were plotted on the same graph in order to juxtapose and observe the effect that material variability has on the deflection of these rods. The function was run for rods of various tapers and various weights. All tapers were retrieved from *David Ray's Taper*

Library (Ray). The taper for each rod can be found in the Appendix. A consistent load and number of nodes was used throughout section 3.4.

3.4.1. TAPERS FOR 7.5 FT 4 WT RODS (STRIP S.D.)

Three different tapers were examined for which the rod was seven and a half feet in length, and was considered to be a 4-weight rod. These rods can be considered to be similar, and were chosen due to their consistencies in weight and length to put emphasis on the effect that taper has on deflection. The tapers for these rods can be seen in the Appendix. For this analysis, we used mean and standard deviation modulus of elasticity values from the strip tensile results, presented in Table 3.1. Three rods were made for each individual taper. One rod was assigned the mean modulus of elasticity value. We will call this the "mean" rod. The second rod was assigned a modulus of elasticity value equal to the mean plus one standard deviation. We will refer to this as the "stiff" rod. The third rod was assigned a modulus of elasticity value equal to the mean minus one standard deviation. We will refer to this rod as the "flexible" rod. The values for elasticity of mean, and mean plus and minus one standard deviation were used to display the extreme conditions in which all six strips that composed the hexagon were of the same elasticity in order to display the potential variability.

The results of this model represent significant variability in deflection in a rod of the same taper based on variability in material. A load of 0.05 lbs was applied to the rods. Observing the range of deflections for each taper, it is apparent that the larger the maximum deflection, the larger the range in deflections. This is true for both vertical and horizontal deflections observed. The range of deflections between the mean plus one standard deviation and the mean minus one standard deviation is 3.7 inches for the

Winston taper. This is significant variability considering that the average deflection under the 0.05 lbs is 13.8 inches.

As mentioned, multiple sources stated that taper is the main and most important factor of fly rod action. When observing the results of how taper effects the deflection of these rods, it is apparent that for a constant value of elasticity there is significant variability across the three different tapers, having a range of 3.18 inches, or 14.1% less than variability in deflection based on material variability. From these findings, it appears that material variability has a significant impact on rod deflection. It is important to re-state that the values for elasticity used represent maximum and minimum values based on standard deviation. This is different from the expected elasticity in rod composed of strips of random elasticity within the standard deviation, which would result in a value closer to the mean, such as represented in the discussion of the results of the transform section model in section 3.3. The results are presented below:

Table 3.4: Tip Deflection of 7.5' Rods (Strip S.D.)

		Deflection (in)		
Taper Name		**Mean**	**Stiff**	**Flexible**
Powell	ΔX	1.79	1.42	2.33
	ΔY	13.01	11.59	14.81
Bernard	ΔX	1.91	1.52	2.46
	ΔY	12.67	11.31	14.37
Winston	ΔX	2.68	2.15	3.42
	ΔY	15.85	14.2	17.9

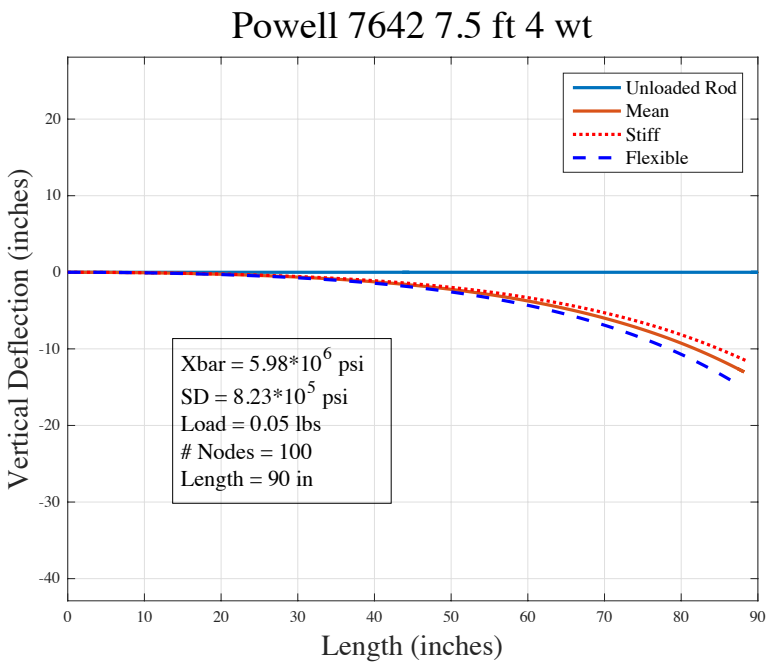

Figure 3.7: Powell taper deflection plot (Strip S.D.)

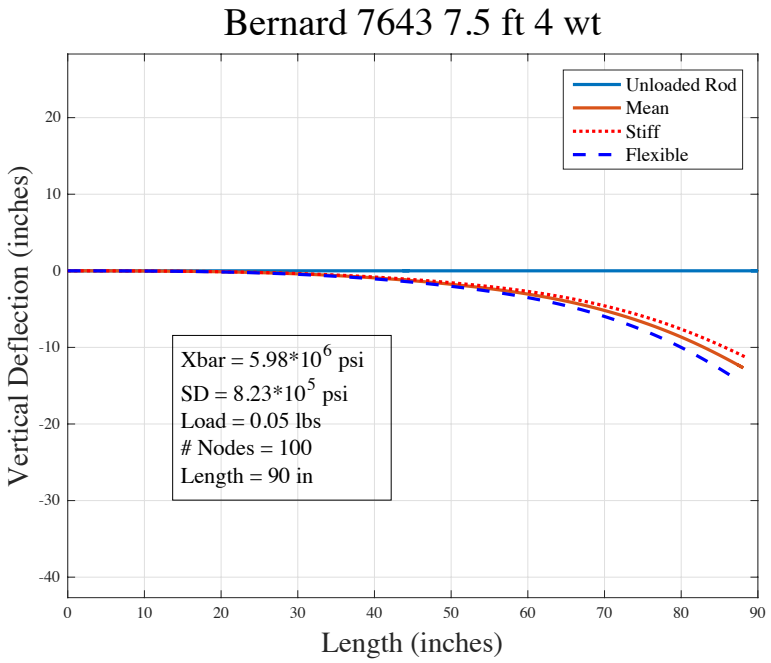

Figure 3.8: Bernard taper deflection plot (Strip S.D.)

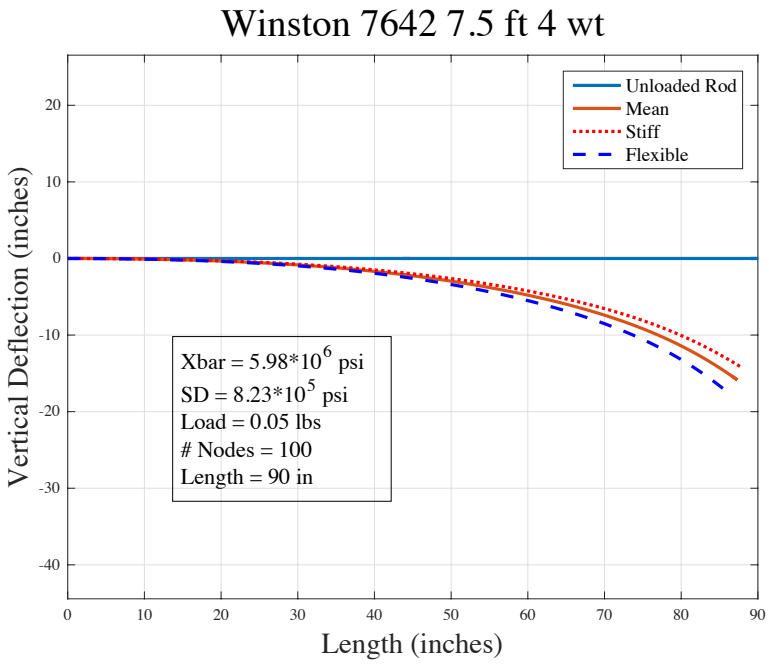

Figure 3.9: Winston taper deflection plot (Strip S.D.)

3.4.2. ADDITIONAL TAPERS

Three additional tapers were observed using the same method as was used for the 7.5-foot long rods. The strip mean modulus of elasticity and standard deviation values were used. Three rods were generated for each taper, consisting of the mean, stiff, and flexible variation as was done in Section 3.4.1. The additional tapers consisted of two 9-foot rods, and one 5-foot rod. These rod tapers can be found in the Appendix. The results are presented below:

Table 3.5: Tip deflection for variety of tapers

Taper Name		Deflection (in)		
		Mean	Stiff	Flexible
Cross Bass	ΔX	0.76	0.59	1.01
	ΔY	9.27	8.19	10.67
Hardy Palakona	ΔX	1.49	1.17	1.95
	ΔY	12.61	11.19	14.41
Mystery	ΔX	1.62	1.29	2.08
	ΔY	10.24	9.15	11.6

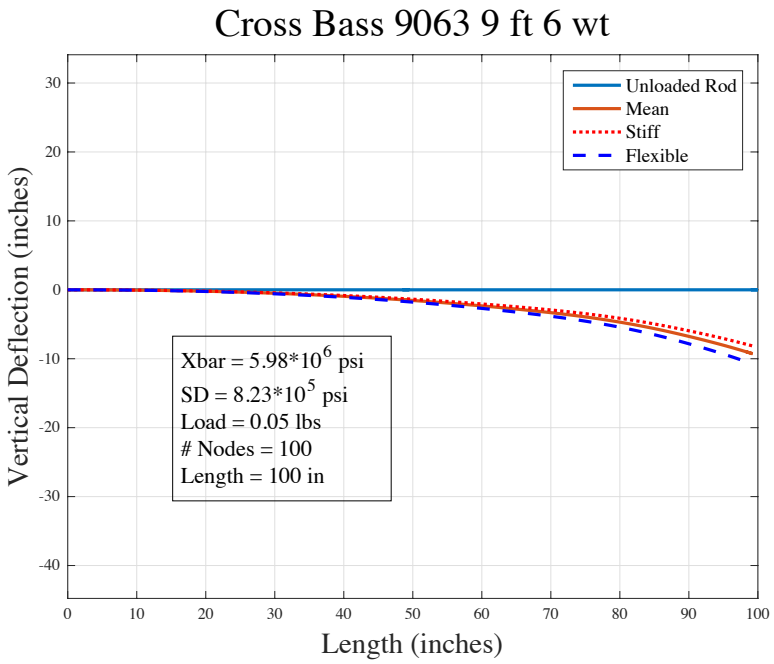

Figure 3.10: Cross Bass taper deflection plot

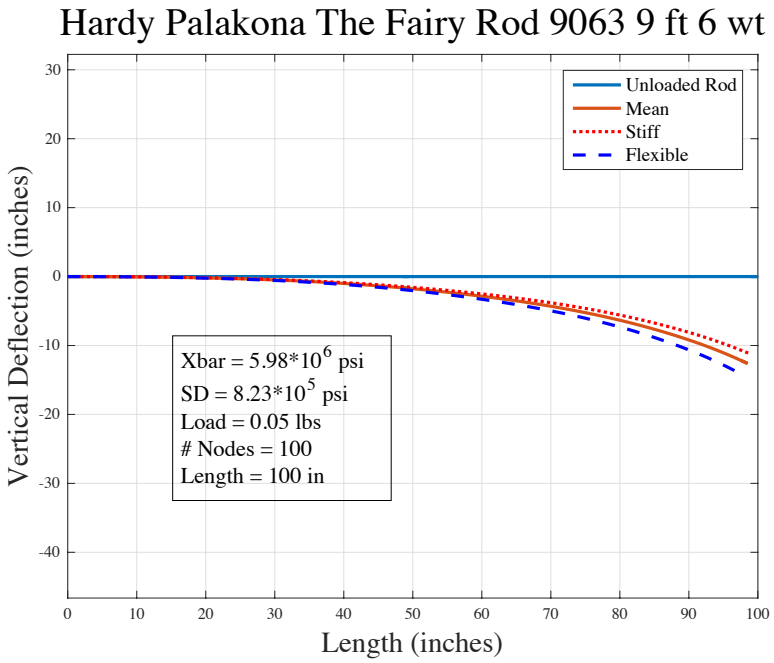

Figure 3.11: Hardy Palakona The Fairy taper plot

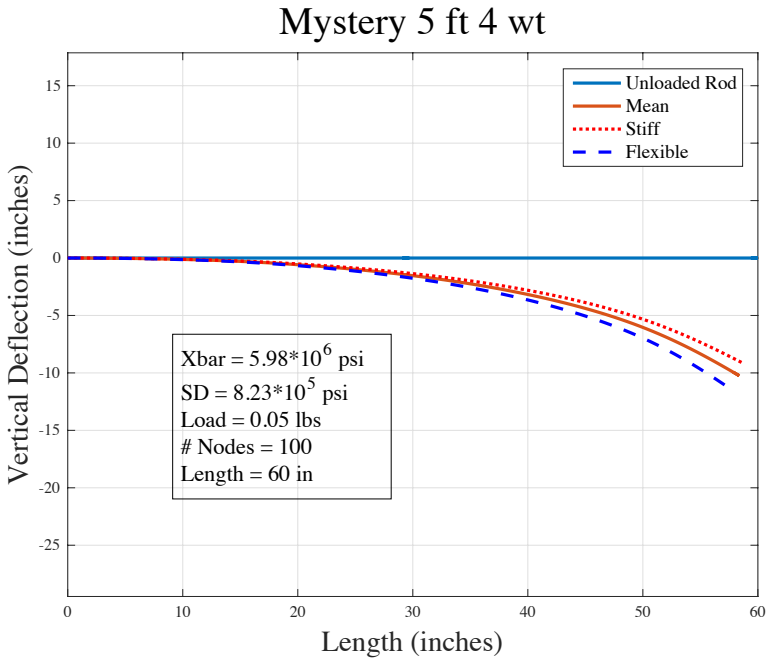

Figure 3.12: Mystery taper plot

Comparing the results from Table 3.4 and Table 3.5 it is evident that a similar relationship exists between variability in modulus of elasticity and variability in rod tip deflection between the six rods analyzed, even with variation in rod length and rod taper.

3.4.3. TAPERS FOR 7.5 FT 4 WT RODS (HEXAGON S.D.)

To produce tip deflection results more representative of what we can expect based on expected effective modulus of elasticity, the hexagon mean and standard deviation values were used. These values are a result of the transform section model and can be found in Table 3.3. The hexagon standard deviation value is approximately half the strip standard deviation due to the averaging effect of the hexagons being comprised of six triangular strips. While the standard deviation used in section 3.4.1 represents the potential that material variability can have on tip deflection variability, the hexagonal standard deviation value should produce a range in tip deflections more representative of

expected results. Three rods were generated for each taper, as was done before, creating a mean, stiff, and flexible rod for each, but with this new standard deviation value.

Observing the Winston taper, we see a range in tip deflection of 2.16 inches. The previous range for the Winston tip deflection when using the strip standard deviation was 3.7 inches. This represents a 41.6% decrease in tip deflection variability between strip standard deviation and hexagon standard deviation. We recall that the range in tip deflection with a constant modulus of elasticity value was 3.18 inches for the Winston taper. We see that taper variability has a 47.2 % greater effect on tip deflection compared to material variability. This is only true when making the assumption that the 2.16-inch range and the 3.18-inch range are accurate representations of the affect of material variability and taper variability on tip deflection. The calculated tip deflections are presented below:

Table 3.6: Tip Deflection of 7.5' Rods (Hexagon S.D.)

Taper Name		**Deflection (in)**		
		Mean	**Stiff**	**Flexible**
Powell	ΔX	1.79	1.56	2.08
	ΔY	13.01	12.14	14.02
Bernard	ΔX	1.91	1.56	2.21
	ΔY	12.67	11.83	13.62
Winston	ΔX	2.68	1.66	3.08
	ΔY	15.85	14.84	17.00

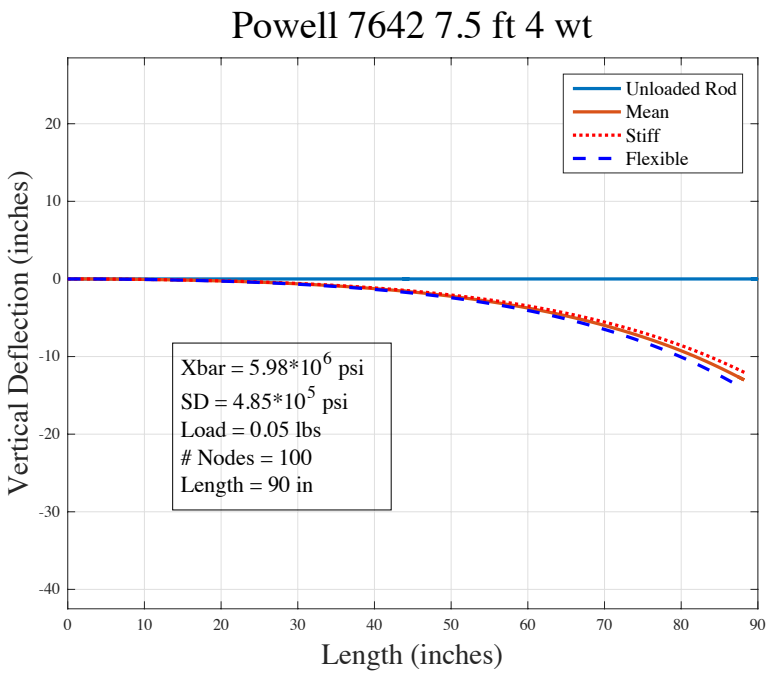

Figure 3.13: Powell taper deflection plot (Hexagon S.D.)

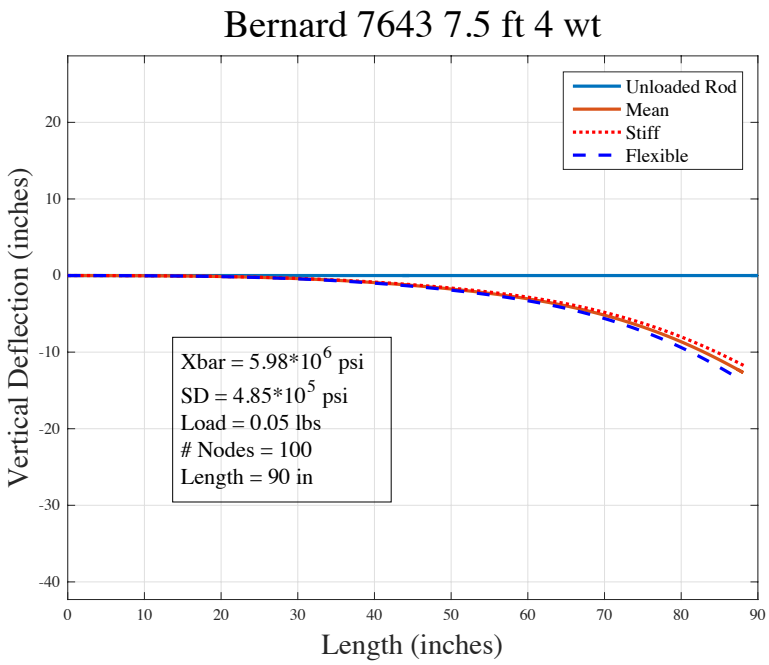

Figure 3.14: Bernard taper deflection plot (Hexagon S.D.)

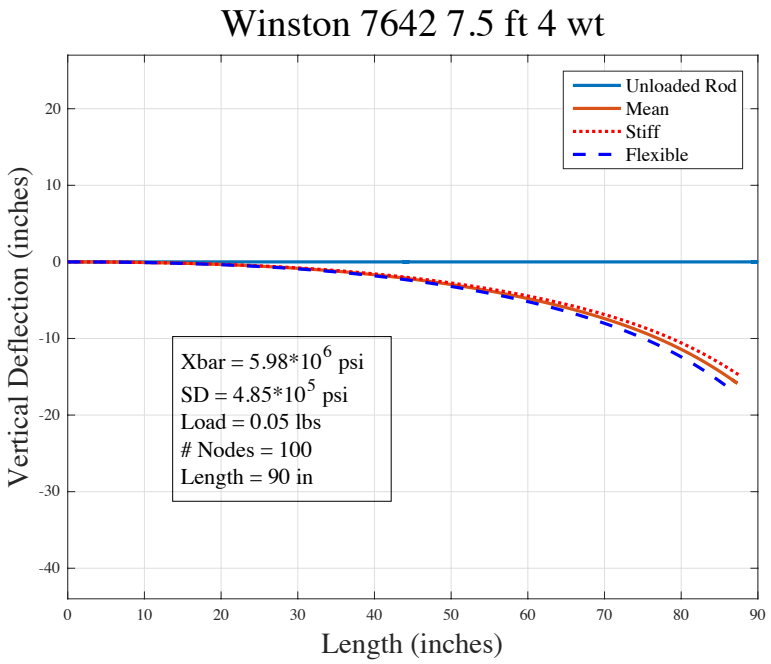

Figure 3.15: Winston taper deflection plot (Hexagon S.D.)

3.4.4. COMPARISON OF ROD TAPERS

In order to demonstrate the effect of rod taper on the deflection of a bamboo fly fishing rod, multiple tapers were plotted on a single graph, all subjected to the same load, and all having the same modulus of elasticity. The three 7.5-foot rod tapers are plotted below:

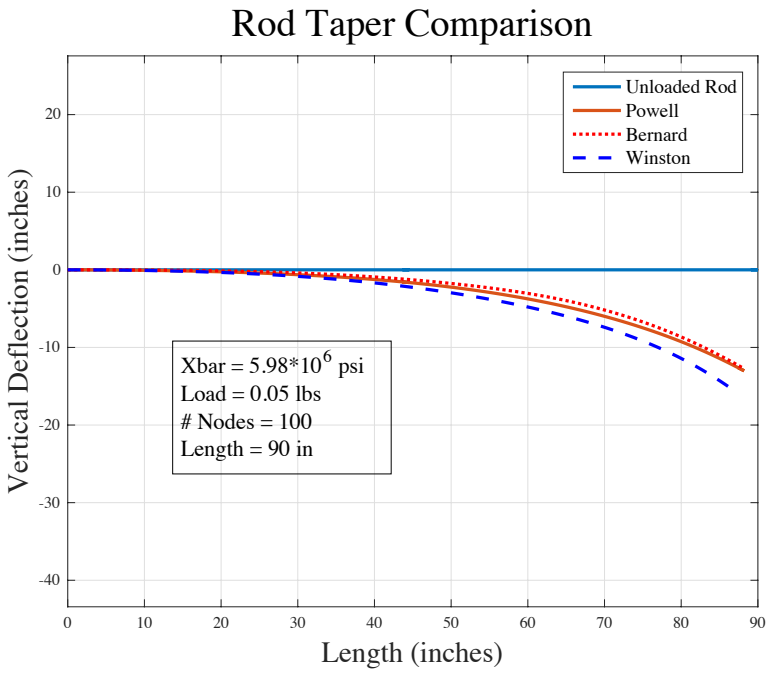

Figure 3.16: Rod taper comparison

Shown above, it is seen that the Powell and Bernard tapers have a similar tip deflection, however have slightly different flexing patterns along the lengths of their rods. The Winston taper experiences a greater tip deflection than the other two tapers, because the cross-sectional area for the Winston taper decreases at a greater rate than the other two tapers displayed.

CHAPTER 4: CONCLUSIONS

Materials testing was performed in order to obtain a range of values for expected bamboo modulus of elasticity. The tensile testing yielded reasonable values for modulus of elasticity, however the 3-point bending test yielded contradicting results. We used the modulus of elasticity values calculated from the tensile testing results in our models.

We compared the effect of material variability and the effect of taper on rod action through two main methods. The first method used the standard deviation value for modulus of elasticity retrieved from the bamboo strip tensile results in the rod deflection function. The result was a range in tip deflections due to material variability 16.4% greater than the range in tip deflections due to taper. This finding is significant when we remember that taper is considered by many to be the dominating factor in rod action. The result of this model represents the potential for material variability to effect rod action, but does not represent the expected outcome. The range in tip deflections produced from variable moduli of elasticity represent an extreme case in which the bounds represent the event in which all six strips of each respective rod have a minimum or maximum modulus of elasticity with respect to one standard deviation based on our materials results. In reality, if six strips are chosen at random, the effective modulus will likely represent a value close to the mean of the strips. Likewise, remembering the results from Table 3.3, it is expected that the combination of these strips into hexagons will effectively reduce the standard deviation by approximately half.

The second method was used to produce a more expected result. In this method, the modulus of elasticity standard deviation value used was the one generated from the transform section function. This is the standard deviation we expect in the hexagonal

bamboo sections after averaging six individual bamboo strips together. When using these values in the rod deflection function, we find that the range in tip deflection due to material variability is 47.2% less than the range in tip deflection due to taper. It is important to note that this is an arbitrary number based on the material testing we conducted, and making the assumption that one standard deviation is a good representation of expected variability. Similarly, the rod tapers were chosen because we consider them to be similar due to their equal lengths and rod weights, however, it is difficult to express the extent to which these rod tapers vary.

We see that the use these two different standard deviation values has a significant effect on the effect of material variability. As stated, the bamboo samples tested likely did not originate from a single culm, however, rod makers generally construct rods out of strips originating from the same culm. Given this fact, it is likely that the effect of material variability on fly rod action is in reality somewhere between the ranges discussed above.

Although a clear relationship between the effect of taper versus the effect of modulus of elasticity on the tip deflection of a bamboo fly rod is not directly made, it is clear that both variables have a significant impact on the vertical deflection of a rod, and therefore, on rod action. This research on the static deflection of a bamboo fly rod completes the first step necessary to being able to accurately model fly rod action and to determine what variables effect this action the most. Future work must consider the dynamic action of a rod. It is also recommended for future work that larger bamboo samples be acquired and tested, and that these samples originate from the same culm, and are all heat treated and maintained at a consistent moisture content. This will give added

insight into material variability within a single culm. The effect of the presence of nodes, the effect of the ratio of dense fibers to pith, the effect of strip location along the culm on modulus of elasticity of the individual strips, and the effect of moisture content is also pertinent information necessary to gaining an understanding of the effect of material variability on a bamboo fly rod. Since many rod makers attempt to construct their rods from a single culm, this will produce more reasonable results for the effect of material variability.

We predict that the use of a single culm to construct individual fly rods will yield a fly rod with strips of similar properties. This would lead to a rod that should behave consistently based on the direction of loading. However, this would likely cause individual rods to be more variable with respect to one another. This is because each culm will have properties different from one another, but strips within a single culm likely have similar properties to a certain extent. Understanding the extent of this variability would be beneficial for rod makers. This would require extensive materials testing to reveal the relationship between bamboo variability within an individual culm versus the variability in bamboo across different culms. If this testing resulted in a clear relationship between the properties of strips within a single culm, the rod maker could use this information and test a strip from a culm and be able to say within some degree of certainty that the rest of the strips taken from that culm would have a properties similar to the tested strip to a certain extent. The rod maker could use this test to predict the properties of a finished rod constructed out of bamboo from that culm.

The moisture content of the bamboo is predicted to be one of the greatest factors in the properties of bamboo. Materials testing with considerations to moisture content

should be done in the future to gain insight into its effect, and how we can manipulate it to gain desired properties. This would open many possibilities for rod makers. For example, if a rod maker wishes to create a rod with a very specific action, he or she would be able to alter the moisture content of individual strips to gain the desired properties. This process might not be practical or cost effective in most situations, but it is likely something we would be capable of given the results of the aforementioned testing.

Combined with a better understanding of bamboo variability retrieved from the proposed materials testing, a dynamic model for fly rod action would give rod makers great insight into how they can alter their practices in order to construct fly rods with desired properties.

BIBLIOGRAPHY

Admin, A. (2009, July). History of Fly Rods. Retrieved October 12, 2017, from http://www.bestflyrods.com/history-of-fly-rods/

Bisshopp, K., & Drucket, D. (1945). Large Deflection of Cantilever Beams, 3(3).

Cameron, J. (n.d.) Bamboo Fly Rods. Retrieved October 23, 2017, from http://www.johncameroncabinetmaker.com/namboo-fly-rods.html

Charles F. [From Old Catalog] Johnson. (1893). Fly fishing for trout and bass. doi:10.5962/bhl.title.34346

Fan, H., & Fan, C. (n.d.). *Test Methods for Determination of Mechanical Properties of Bamboo* [Scholarly project]. Retrieved from http://timber.ce.wsu.edu/resources/papers/P70.pdf

Kretchman, F. (2017, March). Bamboo Fly Rod Questions [Personal interview].

Monahan, P. (2016, May 03). A Beginner's Guide to Bamboo Fly Rods. Retrieved October 07, 2017, from http://www.orvis.com/news/fly-fishing/bamboo-fly-rod-primer/

Ray, D. (n.d.). David Ray's Taper Library. Retrieved October 12, 2017, from http://hexrod.net/Tapers/drtapers/index.html

Schott, W. (2006). *Bamboo in the Laboratoty* [Scholarly project]. Retrieved from http://www.powerfibers.com/BAMBOO_IN_THE_LABORATORY.pdf

Sweetgrass Rods. (n.d.). From Pole to Rod - Our Building Process. Retrieved October 07, 2017, from http://www.sweetgrassrods.com/index.php/hmenu-custom-boo-rods/from-pole-to-rod#!finishing1ss

APPENDIX A – TAPER DIMENSIONS

Powell 7642 7.5 Ft 4 Wt

Rod Name	Powell 7642
Length (inches)	90
Length (feet)	7.5
Line Weight	4
Number of pieces	2
Number of tips	0
Construction	Hex
Comments	
Deduction for varnish	0
Allowance for form setting	0
Ferrule 1 0/64 Location	0

Station Dimension Form Setting

0	0.070	0.035
5	0.084	0.042
10	0.101	0.051
15	0.117	0.059
20	0.130	0.065
25	0.141	0.071
30	0.155	0.078
35	0.164	0.082
40	0.180	0.090
45	0.190	0.095
50	0.206	0.103
55	0.222	0.111
60	0.238	0.119
65	0.254	0.127
70	0.272	0.136
75	0.287	0.144
80	0.301	0.151
85	0.307	0.154
90	0.307	0.154

Bernard 7643 7.5 Ft 4 Wt

Rod Name	Bernard 7643
Length (inches)	90
Length (feet)	7.5
Line Weight	4
Number of pieces	3
Number of tips	1
Construction	Hex
Comments	
Deduction for varnish	0
Allowance for form setting	0
Ferrule 1 0/64 Location	0
Ferrule 2 0/64 Location	0

Station Dimension Form Setting

0	0.073	0.037
5	0.085	0.043
10	0.098	0.049
15	0.109	0.055
20	0.122	0.061
25	0.130	0.065
30	0.145	0.073
35	0.168	0.084
40	0.190	0.095
45	0.200	0.100
50	0.215	0.108
55	0.225	0.113
60	0.234	0.117
65	0.257	0.129
70	0.269	0.135
75	0.281	0.141
80	0.378	0.189
85	0.378	0.189
90	0.378	0.189

Winston 7642 7.5 Ft 4 Wt

Rod Name	Winston 7642
Length (inches)	90
Length (feet)	7.5
Line Weight	4
Number of pieces	2
Number of tips	1
Construction	Hex
Comments	
Deduction for varnish	0
Allowance for form setting	0
Ferrule 1 0/64 Location	0

Station Dimension Form Setting

0	0.058	0.029
5	0.075	0.038
10	0.091	0.046
15	0.105	0.053
20	0.121	0.061
25	0.135	0.068
30	0.154	0.077
35	0.163	0.082
40	0.178	0.089
45	0.187	0.094
50	0.199	0.100
55	0.205	0.103
60	0.219	0.110
65	0.235	0.118
70	0.247	0.124
75	0.259	0.130
80	0.286	0.143
85	0.286	0.143
90	0.286	0.143

Mystery 5' 4wt 5 Ft 4 Wt

Rod Name	Mystery 5' 4wt
Length (inches)	60
Length (feet)	5
Line Weight	4
Number of pieces	0
Number of tips	0
Construction	Hex
Comments	This is a highly spe with only a couple f
Deduction for varnish	0
Allowance for form setting	0

Station Dimension Form Setting

0	0.068	0.034
5	0.076	0.038
10	0.086	0.043
15	0.105	0.053
20	0.125	0.063
25	0.140	0.070
30	0.156	0.078
35	0.172	0.086
40	0.184	0.092
45	0.184	0.092
50	0.215	0.108
55	0.235	0.118
60	0.235	0.118

Cross Bass 9063 9 Ft 6 Wt

Rod Name	Cross Bass 9063
Length (inches)	108
Length (feet)	9
Line Weight	6
Number of pieces	3
Number of tips	1
Construction	Hex
Comments	
Deduction for varnish	0
Allowance for form setting	0
Ferrule 1 0/64 Location	0
Ferrule 2 0/64 Location	0

Station	Dimension	Form Setting
0	0.078	0.039
5	0.095	0.048
10	0.113	0.057
15	0.126	0.063
20	0.141	0.071
25	0.153	0.077
30	0.176	0.088
35	0.221	0.111
40	0.228	0.114
45	0.239	0.120
50	0.249	0.125
55	0.256	0.128
60	0.264	0.132
65	0.279	0.140
70	0.284	0.142
75	0.292	0.146
80	0.300	0.150
85	0.306	0.153
90	0.326	0.163
95	0.336	0.168
100	0.336	0.168

Hardy Palakona The Fairy Rod 9063 9 Ft 6 Wt

Rod Name	Hardy Palakona The Fairy Rod 9063
Length (inches)	108
Length (feet)	9
Line Weight	6
Number of pieces	3
Number of tips	1
Construction	Hex
Comments	18 Ferrule may work better. Signed 'T
Deduction for varnish	0
Allowance for form setting	0
Ferrule 1 12/64 Location	0
Ferrule 2 18/64 Location	0

Station	Dimension	Form Setting
0	0.067	0.034
5	0.082	0.041
10	0.105	0.053
15	0.125	0.063
20	0.134	0.067
25	0.150	0.075
30	0.162	0.081
35	0.178	0.089
40	0.200	0.100
45	0.208	0.104
50	0.217	0.109
55	0.226	0.113
60	0.232	0.116
65	0.244	0.122
70	0.250	0.125
75	0.284	0.142
80	0.296	0.148
85	0.306	0.153
90	0.322	0.161
95	0.337	0.169
100	0.359	0.180

APPENDIX B - MATLAB SCRIPT

I. Rod Deflection Function

```
function [X,Y,Xo,Yo,Yf,Xf] = taper_defl(p,n,E)
%Function for finding equilibrium deflected shape of a beam

taper = xlsread('taper_powell.xlsx');
station = taper(1:end,1);            %Length
dimen = taper(1:end,2);              %Height
l =station(length(station));

li = linspace(0,l,n)';
Hi = interp1q(station, dimen, li);   %Linear interpolation of taper

for i = 1:n-1
    I(i) = 0.0601407 * Hi(i)^4;      %Moment of inertia calculation
end

EI = E * I;
EI = EI';

theta(1) = 0;

ds = l/(n-1);           % Length of single beam segment

tol = 0.1;              % Percent change from previous iteration
change_tip = 2*tol;     % Arbitrary value to force loop at least once

X = li;                 %Initial cantilever beam shape
Y = zeros(1,n);

Xo = li;                %Initial cantilever beam shape for use in plot
Yo = zeros(1,n);

old_tip = 0;            % Initial deflection (before load applied)

% using a while loop to search for equilibrium postion of beam.
% Equilibrium is when curvatures due to moments based on actual beam
shape
% predict the actual deflected shape

while change_tip > tol
    %determine curvature
    %determine slopes
    %determine points

    for i = 1:n-1
        curv(i) = p*(X(n) - X(i))/EI(i);
    end
    for i = 2:n
        theta(i) = curv(i-1)*ds + theta(i-1);
        X(i) = X(i-1) + ds*cos(theta(i-1));
        Y(i) = Y(i-1) - ds*sin(theta(i-1));
    end
```

```
    new_tip = Y(n);
    change_tip = 100*abs((new_tip-old_tip)/old_tip);
    old_tip = new_tip;

end

Yf = -Y(n);   %Final X and Y coordinates of tip
Xf = X(n);
```

II. Rod Deflection Script

```
Xbar = 5.988*10^6;
SD = 8.23*10^5;
p = 0.05;
n = 100;

   E = [Xbar,Xbar + SD,Xbar - SD];
   %RUNS taper_defl TO CREATE DEFLECTION VECTORS FOR EACH VALUE OF E
   [X1,Y1,Xo,Yo,Yf1,Xf1] = taper_defl(p,n,E(1));
     [X2,Y2,Xo,Yo,Yf2,Xf2] = taper_defl(p,n,E(2));
      [X3,Y3,Xo,Yo,Yf3,Xf3] = taper_defl(p,n,E(3));

%PLOT
figure(1);
plot(Xo,Yo,X1,Y1,X2,Y2,'r:',X3,Y3,'b--','LineWidth',2);
grid on;

%LABELS
title('Cross Bass 9063 9 ft 6 wt','fontsize',24);
xlabel('Length (inches)','fontsize',18);
ylabel('Vertical Deflection (inches)','fontsize',18);
axis equal;
%set(figure(1));
lgd = legend('Unloaded Rod','Mean', 'Stiff', 'Flexible');
lgd.FontSize = 12;

%TEXT BOX 1
dim = [0.25 0.25 0.25 0.25];
str = {'Xbar = 5.98*10^6 psi','SD = 8.23*10^5 psi','Load = 0.05 lbs','#
Nodes = 100','Length = 100 in'};
annotation('textbox',dim,'String',str,'FitBoxToText','on','FontSize',14
)

%CHANGE IN X
dX1 = 90 - Xf1;
dX2 = 90 - Xf2;
dx3 = 90 - Xf3;
```

III. Unused Rod Deflection Function

```
function [large_defl,Xl] = large_defl_func(p,l,n,EI)
% script for finding equilibrium deflected shape of a beam.  This uses
% exact curvature instead of approximation.

EI = EI*ones(1,n-1);      %Assuming E is constant

ds = l/(n-1);             % length of single beam segment

tol = 0.1;                % percent change from previous iteration
change_tip = 2*tol;       % arbitrary value to force loop at least once

% intial beam shape
X = linspace(0,l,n);
Y = zeros(1,n);

old_tip = 0;              % initial deflection (before load applied)

% using a while loop to search for equilibrium postion of beam.
% Equilibrium is when curvatures due to moments based on actual beam
shape predict the actual deflected shape

yp(1) = 0;      % at root of cantilever, slope is zero.

while change_tip > tol
    %determine curvature
    %determine slopes
    %determine points
    for i = 1:n-1
        curv(i) = p*(X(n) - X(i))/EI(i);
    end
     ypp(1) = curv(1);
    for i = 2:n
        yp(i) = ypp(i-1)*ds + yp(i-1);
        ypp(i) = curv(i-1)*(1 + yp(i)^2)^(3/2);

        X(i) = X(i-1) + ds*cos(yp(i-1));
        Y(i) = Y(i-1) - ds*sin(yp(i-1));
    end
    new_tip = Y(n);
    change_tip = 100*abs((new_tip-old_tip)/old_tip);
    old_tip = new_tip;

end

large_defl = -Y(n);
Xl = X(n);
```

IV. Transform Section Function

```
function [EI, Ihex] = transformsection( b, n, E1, E2, E3, E4, E5, E6 )

% Dimension analysis for triangles: [1,3,5]

B=linspace(0,b,n+1);                    %B = width(base) for (1,3,5)
H=(b*sqrt(3)/2)/n;                      %H = height of each section

for i = 1:n                             %W=Effective width of rectangles
        W(i) = (B(i+1) + B(i))/2;
end

A=W*H;                                  %A=Area for 1,3,5

% Dimension analysis for triangles: [2,4,6]

V=linspace(b,0,n+1);                    %V= width(base) for (2,4,6)

for i = 1:n                             %C=Effective widths for 2,4,6
        C(i) = (V(i+1) + V(i))/2;
end

S=C*H;                                  %S=Area for 2,4,6

%BOT=Resultant moduli of elasticity for each section of lower half of
hexagon
for i = 1:n
   BOT(i) = (A(i)*E1 + S(i)*E2 + A(i)*E3) / (2*(A(i)) + S(i));
end

%TOP=Resultant moduli of elasticity for each section of upper half of
hexagon
for i = 1:n
   TOP(i) = (S(i)*E4 + A(i)*E5 + S(i)*E6) / ((A(i)) + 2*S(i));
end

%Divides each piece of BOT by selected E, giving ratios

for i = 1:n
    NBOT(i) = BOT(i)/BOT(1);          %NBOT = n value for bottom
end

%Divides each piece of TOP by selected E, giving ratios

for i = 1:n
    NTOP(i) = TOP(i)/BOT(1);          %NTOP = n value for top
end

for i = 1:n
    TWBOT(i)=((2*W(i))+C(i))*NBOT(i);  %TWBOT=Transformed width for bot
    TWTOP(i)=((2*C(i))+W(i))*NTOP(i);  %TWTOP=Transformed width for top
end
```

```
TW=[TWBOT,TWTOP];

TA=TW*H;

%Standard method for finding I
for i=1:2*n
    Y(i)=(.5*H)+(H*(i-1));
end

for i =1:2*n
    AY(i)=TA(i)*Y(i);
end

YNA=sum(AY)/sum(TA);

for i=1:2*n
    Yi(i)=(Y(i)-YNA)^2;
    Io(i)=(1/12)*TW(i)*H^3;
    Ii(i)=TA(i)*Yi(i);
end

E=BOT(1);
I=sum(Ii)+sum(Io);
EI = E*I;

Ihex = 0.5412659 * b^4;

E = EI / Ihex;

end
```

AUTHOR'S BIOGRAPHY

Bennett R. Scully was born in Damariscotta, Maine, on March 16, 1996. He was raised in Edgecomb, Maine and graduated from Boothbay Region High School in 2014. Bennett majors in civil & environmental engineering. He is a member of Alpha Tau Omega. Bennett plans to pursue a career Maine in the field of civil engineering.